Published in final edited form as:

Gastroenterology. 2020 October ; 159(4): 1342–1356.e6. doi:10.1053/j.gastro.2020.06.049.

Intestinal Epithelial Expression of MHCII Determines Severity of Chemical, T-Cell–Induced, and Infectious Colitis in Mice

Deepa R. Jamwal[1], **Daniel Laubitz**[1], **Christy A. Harrison**[1], **Vanessa Figliuolo da Paz**[1], **Christopher M. Cox**[2], **Rachel Wong**[3], **Monica Midura-Kiela**[1], **Michael A. Gurney**[1], **David G. Besselsen**[4], **Prashanth Setty**[1], **Lonnie Lybarger**[2], **Deepta Bhattacharya**[3], **Jean M. Wilson**[2], **Fayez K. Ghishan**[1,§], **Pawel R. Kiela**[1,3,§]

[1]Department of Pediatrics, University of Arizona, Tucson, Arizona

[2]Department of Cellular and Molecular Medicine, University of Arizona, Tucson, Arizona

[3]Department of Immunobiology, University of Arizona, Tucson, Arizona

[4]University Animal Care, University of Arizona, Tucson, Arizona

Abstract

BACKGROUND & AIMS: Intestinal epithelial cells (IECs) provide a barrier that separates the mucosal immune system from the luminal microbiota. IECs constitutively express low levels of major histocompatibility complex (MHC) class II proteins, which are upregulated upon exposure to interferon gamma. We investigated the effects of deleting MHCII proteins specifically in mice with infectious, dextran sodium sulfate (DSS)-, and T-cell–induced colitis.

METHODS: We disrupted the histocompatibility 2, class II antigen A, beta 1 gene (*H2-Ab1*) in IECs of C57BL/6 mice (I-Ab$^{\Delta IEC}$) or *Rag1*$^{-/-}$ mice (*Rag1*$^{-/-}$I-Ab$^{\Delta IEC}$); we used I-Ab^{WT} mice as controls. Colitis was induced by administration of DSS, transfer of CD4^{+}CD45RB^{hi} T cells,

Address correspondence to: Pawel R. Kiela, DVM, PhD, Department of Pediatrics, University of Arizona, Steele Children's Research Center, 1501 N. Campbell Ave., Tucson, AZ 85724. pkiela@peds.arizona.edu.

[§]Authors share co-senior authorship.

CRediT Authorship Contributions

Deepa R. Jamwal, PhD (Formal analysis: Lead; Investigation: Lead; Methodology: Lead; Writing – original draft: Lead; Writing – review & editing: Supporting). Daniel Laubitz, PhD (Data curation: Supporting; Formal analysis: Equal; Methodology: Supporting; Software: Supporting; Visualization: Supporting; Writing – review & editing: Supporting). Christy A. Harrison, PhD (Formal analysis: Supporting; Investigation: Supporting). Vanessa Figliuolo da Paz, PhD (Formal analysis: Supporting; Investigation: Supporting; Visualization: Supporting; Writing – review & editing: Supporting). Christopher M. Cox, PhD (Investigation: Supporting; Writing – review & editing: Supporting). Rachel Wong, BS (Formal analysis: Supporting; Investigation: Supporting; Writing – review & editing: Supporting). Monica Midura-Kiela, MS (Investigation: Supporting). Michael A. Gurney, PhD (Investigation: Supporting). David G. Besselsen, DVM, PhD (Formal analysis: Supporting; Investigation: Supporting). Prashanth Setty, PhD (Investigation: Supporting). Lonnie Lybarger, PhD (Formal analysis: Supporting; Investigation: Supporting; Writing – review & editing: Supporting). Deepta Bhattacharya, PhD (Data curation: Supporting; Funding acquisition: Supporting; Investigation: Supporting; Validation: Supporting; Writing – review & editing: Supporting). Jean M. Wilson, PhD (Funding acquisition: Supporting; Investigation: Supporting; Supervision: Supporting; Writing – review & editing: Supporting). Fayez K. Ghishan, MD (Conceptualization: Supporting; Funding acquisition: Supporting; Supervision: Supporting; Writing – review & editing: Supporting). Pawel R Kiela, DVM, PhD (Conceptualization: Lead; Data curation: Supporting; Formal analysis: Supporting; Funding acquisition: Lead; Investigation: Supporting; Supervision: Lead; Visualization: Supporting; Writing – original draft: Equal; Writing – review & editing: Lead)

Supplementary Material

Note: To access the supplementary material accompanying this article, visit the online version of *Gastroenterology* at www.gastrojournal.org, and at https://doi.org/10.1053/j.gastro.2020.06.049.

Conflict of interest

The authors disclose no conflicts.

or infection with *Citrobacter rodentium*. Colon tissues were collected and analyzed by histology, immunofluorescence, xMAP, and reverse-transcription polymerase chain reaction and organoids were generated. Microbiota (total and immunoglobulin [Ig]A-coated) in intestinal samples were analyzed by16S amplicon profiling. $IgA^{+}CD138^{+}$ plasma cells from Peyer's patches and lamina propria were analyzed by flow cytometry and IgA repertoire was determined by next-generation sequencing.

RESULTS: Mice with IEC-specific loss of MHCII ($I\text{-}Ab^{DIEC}$ mice) developed less severe DSS- or T-cell transfer-induced colitis than control mice. Intestinal tissues from $I\text{-}Ab^{\Delta IEC}$ mice had a lower proportion of IgA-coated bacteria compared with control mice, and a reduced luminal concentration of secretory IgA (SIgA) following infection with *C rodentium*. There was no significant difference in the mucosal IgA repertoire of $I\text{-}Ab^{\Delta IEC}$ vs control mice, but opsonization of cultured *C rodentium by* SIgA isolated from $I\text{-}Ab^{\Delta IEC}$ mice was 50% lower than that of SIgA from mAb^{WT} mice. Fifty percent of $I\text{-}Ab^{\Delta IEC}$ mice died after infection with *C rodentium*, compared with none of the control mice. We observed a transient but significant expansion of the pathogen in the feces of $I\text{-}Ab^{\Delta IEC}$ mice compared with $I\text{-}Ab^{WT}$ mice.

CONCLUSIONS: In mice with DSS or T-cell–induced colitis, loss of MHCII from IECs reduces but does not eliminate mucosal inflammation. However, in mice with *C rodentium*–induced colitis, loss of MHCII reduces bacterial clearance by decreasing binding of IgA to commensal and pathogenic bacteria.

Keywords

Antigen Presentation; Immune Regulation; Antibody Production; Activation

---

The gastrointestinal tract is exposed to a barrage of bacterial and dietary antigens. At steady-state, the mucosal immune response is subdued and balanced, thus averting an unchecked and chronic inflammatory response. Breakdown of the suppressed/tolerogenic tone in the gut leads to inflammatory bowel disease (IBD), including Crohn's disease (CD) and ulcerative colitis. A single cell layer of intestinal epithelial cells (IECs) provides the primary interface in the gastrointestinal tract that not only acts as the physical barrier isolating the microbes from the host but also plays a vital role in maintaining immune homeostasis.[1,2]

IECs also directly influence T-cell activity in their capacity to act as antigen presenting cells (APC).[1,3] At homeostasis, small intestinal IECs constitutively express low levels of MHCII, hallmark molecules of APCs.[4,5] Interferon (IFN)γ causes a dramatic up-regulation of MHCII by IECs, both in vitro and in vivo.[6,7] Elevated IEC expression of MHCII has been confirmed in biopsies from inflamed small and large intestines in IBD[3] and celiac disease.[8] Cellular localization of MHCII in the polarized IECs has not been described consistently, with predominantly apical expression[5,9] or lateral and basolateral localization.[10,11] MHCII is redistributed in the inflamed epithelium from multivesicular bodies to the basolateral membrane.[10] When coincident with increased expression of co-stimulatory CD86[12] and CD40,[13] this process has been postulated to allow IECs to modulate immune responses during an infectious or inflammatory insult, by presenting antigens to promote pathogen clearance or immune tolerance.

The functional role of MHCII at steady-state and during inflammation has largely been studied in cell lines and primary cells obtained from rodent and human colons.[6,14,15] Primary mouse colonic epithelial cells (CECs), not stimulated to express MHCII, could not activate $CD4^+$ T cells and suppressed macrophage-induced $CD4^+$ T-cell activation.[14] Contrarily, rat IECs from the small intestine (a site of low constitutive MHCII expression) induced strong proliferation of primed $CD4^+$ T but not naïve $CD4^+$ T cells,[15] and coculture with a human IEC cell line resulted in significant T-cell activation.[6] As compared with healthy controls, IECs from patients with IBD were either highly efficient at inducing $CD4^+$ T-cell polarization,[2] or at inducing T-cell anergy,[16] suggesting that IECs may behave differently during inflammation than in health. MHCII expression in IECs has been implicated in the initiation of lethal graft-versus-host disease[17] and $MHCII^+$ $Lgr5^+$ intestinal stem cells have been confirmed to act as nonconventional APCs in cocultures with $CD4^+$ T lymphocytes.[18]

Due to the conflicting results published, it was imperative to study the role of epithelial MHCII in an animal model. However, the models generated so far (ie, transgenic mice with exclusive MHCII expression in IECs[19] or mice with deletion of IFNγ-inducible CIITA promoter pIV in IEC or nonhematopoietic cells)[20] lacked the resolution needed to fully understand the immunomodulatory roles of epithelial MHCII in health and disease. To address this, we generated conditional knockout of MHCII in the intestinal epithelium of C57BL/6 mice ($I\text{-}Ab^{\Delta IEC}$) and studied the mucosal response to epithelial injury, T-cell mediated colitis, and in *Citrobacter rodentium* infectious colitis. While IEC-specific deletion of MHCII conferred protection in DSS and T-cell transfer colitis, it was deleterious in infectious colitis with apparent impairment of B-cell function, reduced luminal IgA avidity, and compromised pathogen clearance.

Materials and Methods

Mice

All mice are described in Supplemental Experimental Procedures. All animal protocols and procedures were approved by the University of Arizona Animal Care and Use Committee protocol (Kiela, 07–126). Villin-Cre^+ $I\text{-}Ab^{fl/fl}$ mice are referred to as $I\text{-}Ab^{\Delta IEC}$, and their Cre^- littermates as $I\text{-}Ab^{WT}$.

Ex Vivo Organoid Culture From Colons and IFN-γ Stimulation

The organoids were prepared and cultured from the colons of $I\text{-}Ab^{WT}$ or $I\text{-}Ab^{\Delta IEC}$ mice as described in detail in the Supplemental Experimental Procedures.

DSS-induced Colitis

Acute colitis was induced in $I\text{-}Ab^{WT}$ or $I\text{-}Ab^{\Delta IEC}$ mice with 3% dextran sodium sulfate (DSS) in the drinking water for 7 days. In a recovery study, a separate cohort of mice was administered 3% DSS for 7 days, switched to normal water, and allowed to recover for 14 days before euthanasia. Mice were monitored daily for the symptoms of colitis, such as body weight loss, lethargy, loss of grooming, and diarrhea.

Adoptive T-Cell Transfer Colitis

$Rag^{-/-}$I-Ab^{WT} and $Rag1^{-/-}$I-$Ab^{\Delta IEC}$ mice were adoptively transferred with naïve $CD4^{+}CD45RB^{Hi}$ T cells as described in detail in the Supplemental Experimental Procedures section.

Citrobacter rodentium Infection

I-Ab^{WT} or I-$Ab^{\Delta IEC}$ mice were orally gavaged with *Citrobacter rodentium* DBS100. For details on bacterial preparation see Supplemental Experimental Procedures. Mice were monitored for symptoms of colitis such as body weight loss, lethargy, loss of grooming, and diarrhea. Fecal samples were collected longitudinally and stored at −°C for lipocalin-2 quantification and microbiota analysis. Blood samples were collected from the tail vein of mice and serum was stored at −80°C until use. Fecal lipocalin-2, intestinal secretory IgA (SIgA), and serum amyloid A were detected by enzyme-linked immunosorbent assay (ELISA) (R&D Systems, Bio-Techne Corporation, Minneapolis, MN) according to the manufacturer's instructions. For details on sample preparation see Supplemental Experimental Procedures. Mice were euthanized on day 9 or 21 postinfection for tissue collection. Details on histology, immunofluorescence, and quantitative reverse-transcriptase polymerase chain reaction (qRT-PCR) are provided in the Supplemental Experimental Procedures.

Fecal Microbial DNA Extraction and Microbiome Analysis

DNA from fecal samples was extracted using the DNeasy PowerSoil HTP 96 Kit (Qiagen. Hilden, Germany) according to the manufacturer's protocol. For details on library preparation and 16s amplicon profiling, see Supplemental Experimental Procedures.

Colonic Explant Culture and xMAP Assays

To evaluate the production of mucosal cytokines, colonic segments were cultured for 24 hours, after which time, the supernatants were collected and stored for multiplex cytokine analysis using MagPix (Luminex, Austin, TX). For more details, see Supplemental Experimental Procedures.

Flow Cytometry/Sorting of IgA-Coated Bacteria and Secretory IgA Analysis

Bacteria from colon, ileum, and cecum of I-Ab^{WT} and I-$Ab^{\Delta IEC}$ mice were stained with fluorescein isothiocyanate anti-mouse IgA (BD Pharmingen, San Jose, CA) and *Bac*Light™ Red Bacterial Stain (Thermo Fisher, Waltham, MA) and evaluated by flow cytometry. IgA-coated bacteria were flow-sorted (BD FACS ARIA III), and DNA was extracted and used for 16S amplicon library generation and sequencing. For details on sample preparation see Supplemental Experimental Procedures. In some experiments, mucosal scrapings and intestinal luminal washings were used for quantification of SIgA via ELISA (TSZ ELISA, Biotang USA, Albuquerque, NM).

C rodentium–IgA Binding Assay

SIgA from the ileum of I-Ab^{WT} or I-$Ab^{\Delta IEC}$ mice was allowed to bind with *C rodentium* DBS100. For details on this experiment see Supplemental Experimental Procedures.

Gene Microarray Analysis

Colon tissue samples from uninfected I-Ab^{WT} and I-Ab$^{\Delta IEC}$ mice were used for microarray gene expression analysis using GeneChipMouse Gene 2.0 ST arrays (Thermo Fisher; details in Supplemental Experimental Procedures).

IgA Repertoire Analysis

IgA^{+}CD138^{+} cells were isolated from small intestinal lamina propria and Peyer's patches (PPs) of I-Ab^{WT} and I-Ab$^{\Delta IEC}$ mice using Flow Sorting and were subjected to Somatic Hypermutation Analysis (details in Supplemental Experimental Procedures).

Antibodies and Primers

Antibodies and primers used in the course of the projects are listed in the Supplementary Tables 1, 2 and 3, respectively.

Statistical Analysis

Data are expressed as the means ± standard deviation. Statistical analysis was performed using Graph Pad Prism version 7.0 for Windows (Graph Pad Software, San Diego, CA). Data distribution was evaluated with Shapiro-Wilk test and analyzed by analysis of variance, unpaired Student *t* test, or Mann-Whitney *t* test, as appropriate. Bonferroni multiple comparison test was used where applicable. Bioinformatics of microbiome and IgA repertoire analysis are described in detail in the Supplemental Experimental Procedures.

Results

MHCII Is Upregulated in CECs in Experimental Colitis

To verify MHCII expression in the inflamed colon, we induced colitis in immunodeficient Rag1 $^{-/-}$ mice by adoptively transferring naïve CD4^{+}CD45RB^{hi} T cells. T-cell–transferred Rag1$^{-/-}$ mice developed inflammation within 8 weeks, as indicated by an increase in inflammatory infiltrate in the colonic lamina propria (cLP) along with an increase in mucosal inflammatory cytokine expression (Figure 1A). In PBS-injected Rag1$^{-/-}$ mice, MHCII expression was limited to the LP, presumably resident cLP macrophages, and dendritic cells (DCs), whereas the development of colitis was associated with a strongly induced expression of MHCII along the basolateral membrane and highly fluorescent puncta within the sub-apical compartment (Figure 1B).

Mouse Model of Conditional Knockout of I-A^{b} in the Intestinal Epithelium

To assess the importance/contribution of MHCII expression in IECs in mucosal immune homeostasis/inflammation, we generated conditional C57BL/6J knockout mice with disrupted H2-Ab1 gene in the IEC (I-Ab$^{\Delta IEC}$). (I-Ab^{WT} mice were used as controls. I-Ab$^{\Delta IEC}$ mice were born and weaned at the expected Mendelian ratio and did not display an overt phenotype. Loss of epithelial MHCII was first confirmed using immunofluorescence in colonic sections of Rag1$^{-/-}$I-Ab^{WT} or Rag1$^{-/-}$I-Ab$^{\Delta IEC}$ mice adoptively transferred with naïve T cells to induce colitis and epithelial MHCII expression. Contrary to Rag1$^{-/-}$I-Ab^{WT} mice, no visible IEC-specific signal was observed in the inflamed colons of Rag1$^{-/-}$I-

$Ab^{\Delta IEC}$ mice (Figure 1C). To further confirm deletion of the I-Ab gene in the IECs, we cultured colonic organoids from I-Ab^{WT} and I-$Ab^{\Delta IEC}$ mice with/without IFNγ for 18 hours, followed by qRT-PCR for I-Ab and CIITA, the IFNγ-inducible Class II MHC Transactivator. On IFNγ exposure, organoids derived from both I-Ab^{WT} and I-$Ab^{\Delta IEC}$ mice significantly upregulated CIITA (Figure 1D). However, organoids from I-$Ab^{\Delta IEC}$ mice failed to up-regulate I-Ab, confirming efficient recombination and inactivation of the H2-Ab1 gene in IECs (Figure 1D).

IEC-specific MHCII Deletion Is Marginally Protective During Acute DSS-induced Colitis But improves Recovery From Mucosal Injury

To test the role of epithelial MHCII in acute mucosal injury, I-Ab^{WT} and I-$Ab^{\Delta IEC}$ mice were subjected to 3% DSS treatment for 7 days. Although both I-Ab^{WT} and I-$Ab^{\Delta IEC}$ mice showed significant weight loss as compared with the control (water only) littermates (Figure 2A), DSS-treated I-$Ab^{\Delta IEC}$ mice tended to lose less weight as compared with I-Ab^{WT} mice (without reaching statistical significance, Figure 2A). However, DSS-treated $Ab^{\Delta IEC}$ mice had significantly lower colon length/weight ratio than their I-Ab^{WT} counterparts, reflecting reduced intestinal inflammation (Figure 2B). Although the DSS-treated I-$Ab^{\Delta IEC}$ mice appeared more active, despite the somewhat improved histology, the persistent mucosal immune infiltration resulted in statistically indistinguishable inflammation scores from that of DSS-treated I-Ab^{WT} mice (Figure 2C).

Consistent with the trend in improved weight and colon length/weight ratio, acute DSS colitis in I-$Ab^{\Delta IEC}$ mice was associated with lower expression of mucosal inflammatory cytokines such as interleukin (IL)1β and IL6 as compared with I-Ab^{WT} mice (Figure 2D). However, there was elevated expression of IL12p40 and IFNγ in DSS-treated I-$Ab^{\Delta IEC}$ mice, whereas tumor necrosis factor (TNF)α increased in both genotypes (Figure 2D).

We assessed the frequency of cLP $CD4^+$ T cells using flow cytometry. Regardless of the genotype, DSS treatment led to a similar increase in the frequency of activated T-helper cells ($CD44^+CD62L^-CD4^+$) in cLP and mesenteric lymph nodes (MLNs) when compared with mice with regular drinking water (Supplementary Figure 1A and B). IECs contribute to the induction and peripheral expansion of $CD4^+CD25^+FoxP3^+$ regulatory T cells (Tregs) in a DC-independent fashion.[21] Under steady-state, we found that I-$Ab^{\Delta IEC}$ mice had slightly, but not significantly, lower frequency of Tregs in the cLP, as compared with I-Ab^{WT} mice (Figure 2E and F). In acute DSS colitis, cLP Tregs significantly decreased in I-Ab^{WT} mice, whereas there was no significant difference between water- and DSS-treated I-$Ab^{\Delta IEC}$ mice (Figure 2E and F). Increased $CD4^+CD25-Foxp3^+$ cells have been associated with various autoimmune pathologies and are sometimes referred to as “unconventional” Tregs.[22] DSS induced a similar expansion in the frequency of cLP $CD25^-$ Tregs in both I-Ab^{WT} and I-$Ab^{\Delta IEC}$ mice (Figure 2E and F). Overall, IEC-specific ablation of MHCII had minor effects on the mucosal effector and regulatory $CD4^+$ T cells.

To determine whether the epithelium contributes to the restitution phase after mucosal injury, mice were treated with 3% DSS for 7 days followed by a 2-week recovery. Both I-Ab^{WT} and I-Ab^{-IEC} mice started to lose weight by day 5 and started to improve by day 12 (Figure 3A). One of 7 I-Ab^{WT} mice died on day 12, whereas all of the I-$Ab^{\Delta IEC}$ mice

survived the experiment (Supplementary Figure 2). At the end of recovery period, colonic histology in I-Ab$^{\Delta IEC}$ mice showed significant improvement (Figure 3B). The improved recovery in I-Ab$^{\Delta IEC}$ mice correlated with decreased mucosal expression of IL1β, IFNγ, and TNFα as compared with I-Ab^{WT} mice (Figure 3C). In colonic explant culture, IFNγ and IL1β showed a trend toward downregulation in I-Ab$^{\Delta IEC}$ mice, and a trend toward increased secretion of IL22, a cytokine demonstrated to promote tissue repair (Figure 3D).[23] IL1β, IFNγ, and TNFα have been associated with exacerbation of DSS colitis in mice.[24] It is plausible that decreased expression of these 3 proinflammatory mediators, compounded by the observed trend for higher mucosal secretion of IL22 offered the observed protection in DSS-treated I-AB$^{\Delta IEC}$ mice.

IEC-specific MHCII Deletion Confers Protection in T-Cell–induced Colitis

To explore the role of epithelial MHCII in T-cell–induced colitis, inflammation was induced in Rag1$^{-/-}$I-Ab^{WT} and Rag1$^{-/-}$I-Ab$^{\Delta IEC}$ mice using adoptive transfer of naïve CD4^{+}CD45RB^{hi} T cells from the spleens of wild-type C57BL/6 mice. By 5 weeks following T-cell transfer, both Rag1$^{-/-}$I-Ab^{WT} and Rag1$^{-/-}$I-Ab$^{\Delta IEC}$ mice started to lose weight. However, while Rag1$^{-/-}$I-Ab^{WT} mice continued to deteriorate, Rag1$^{-/-}$I-Ab$^{\Delta IEC}$ mice began to recover in weeks 6 to 8 (Figure 4A). During this time, most T-cell–transferred Rag1$^{-/-}$I-Ab$^{\Delta IEC}$ mice did not exhibit typical features of colitis such as rough coat, loss of grooming or diarrhea. These findings were not fully reflected in histological improvement, as we observed large individual differences among adoptively transferred Rag1$^{-/-}$I-Ab$^{\Delta IEC}$ mice (Figure 4B). Because of this spread of scores, we could not provide representative hematoxylin-eosin images. However, we observed lower penetrance of colitis in Rag1$^{-/-}$I-Ab$^{\Delta IEC}$ mice, as the percentage of mice with inflammation score of equal or higher to median score (66.6% in adoptively transferred Rag1$^{-/-}$I-Ab^{WT} mice) decreased to 44.4% in Rag1$^{-/-}$I-Ab$^{\Delta IEC}$. qRT-PCR did not detect Foxp3 messenger RNA (mRNA) expression in the colonic mucosa of any of the experimental mice, suggesting minimal conversion of naïve T cells to induced Tregs (iTregs) in this model and no detectable homing to the cLP (not shown). It also excluded the possibility that iTregs could have contributed to the observed variation in colitis severity in these mice. As expected, T-cell transfer in Rag1$^{-/-}$I-Ab^{WT} mice led to a significant increase in colonic IFNγ transcript, but this effect was not different from Rag1$^{-/-}$I-Ab$^{\Delta IEC}$ mice (Figure 4C). IL1β and IL12 (Figure 4C) and IL17a (Supplementary Figure 3A) followed similar trends, although large individual differences affected statistical analysis. TNFα was similarly upregulated in both strains transferred with naïve T cells. In colonic explant culture, we observed somewhat reduced IFN-γ and increased IL22 secretion from the colons of Rag1$^{-/-}$I-Ab$^{\Delta IEC}$ as compared with Rag1$^{-/-}$I-Ab^{WT} mice (Figure 4D), and the expression of RegIIIγ mRNA, a known target of IL22, showed a mild (not significant) increase in the colonic mucosa of Rag1$^{-/-}$I-Ab$^{\Delta IEC}$ mice (Figure 4D). Although there was no difference in the frequency of IL17a producing CD4^{+}T cells in both cohorts of mice (Supplementary Figure 3B), consistent with data on mucosal IFNγ mRNA expression, the frequency of IFNγ-producing CD4^{+} T cells tended to be lower in the cLP of Rag1$^{-/-}$I-Ab$^{\Delta IEC}$ mice (Figure 4E).

IEC-specific MHCII Deletion Increases Susceptibility to Infectious Colitis

We infected I-Ab^{WT} and I-Ab$^{\Delta IEC}$ mice with *C rodentium* and followed them up to 21 days postinfection (Figure 5A). By day 3, all mice started losing weight and, by day 15, 50% of I-Ab$^{\Delta IEC}$ mice had died (Figure 5B). On day 9 postinfection, fecal lipocalin 2, a marker for intestinal inflammation, was significantly higher in the infected I-Ab$^{\Delta IEC}$ mice (Figure 5C). At the same time, serum amyloid A, a protein involved in phagocytic killing of Gram-negative bacteria[25] and protective in experimental colitis,[26] was significantly lower in the blood of I-Ab$^{\Delta IEC}$ mice (Figure 5D). The study was repeated with another cohort of mice and terminated on day 9, before the onset of high mortality. *C rodentium*–infected I-Ab$^{\Delta IEC}$ mice had more severe colonic inflammation than the infected I-Ab^{WT} controls (Figure 5E and F). We measured the expression of RegIIIγ, IL22, IL17A, IL23A, and IL6 (Supplementary Figure 4) on day 9 postinfection. *Citrobacter* infection failed to increase the expression of IL23A and we did not find significant differences in the expression of RegIIIγ IL22, IL17A, and IL6 between *C rodentium*–infected I-AB$^{\Delta IEC}$ and I-AB^{WT} colons (Supplementary Figure 4), thus suggesting that the higher susceptibility of I-Ab$^{\Delta IEC}$ mice to infectious colitis was not due to differential induction of antimicrobial peptides, Th17, or Th22 responses.

Aggravated Colitis in C rodentium–infecfed I-Ab$^{\Delta IEC}$ Mice Is Associated With Transient Uncontrolled Pathogen Expansion

Fecal microbiome 16S profiling showed similar alpha diversity in fecal microbiota of I-Ab^{WT} and I-Ab$^{\Delta IEC}$ mice at the onset of the studies (baseline before antibiotic treatment and infection) (Figure 6A). Alpha diversity dropped in both strains after antibiotic treatment and continued to decrease after *C rodentium* infection (Figure 6A). This decrease was more transient in I-Ab^{WT} mice with near complete recovery by day 21, consistent with the self-resolving nature of *C rodentium* infection. In I-Ab$^{\Delta IEC}$ mice, on days 6 and 9 we observed a more profound decline in alpha diversity after infection compared with the infected I-Ab^{WT} mice (Figure 6A). This was also reflected in beta diversity analysis as indicated in the Bray-Curtis dissimilarity plot with time as the x-axis (Figure 6B). Taxonomic analysis at the genus level indicated that the drop in alpha diversity was associated with the transient expansion of *C rodentium* in both mouse strains, which was more pronounced in the infected I-Ab$^{\Delta IEC}$ mice (Figure 6C). Surviving I-Ab$^{\Delta IEC}$ mice returned to a microbial community comparable to that of infected I-Ab^{WT} by day 21 (Figure 6B). These observations were confirmed by qPCR with primers specific for *C rodentium* espB gene relative to signal for 16s ribosomal RNA universal primers (Figure 6D) and suggested that I-Ab$^{\Delta IEC}$ mice were not able to control the pathogen as effectively as I-Ab^{WT} littermates. These findings were validated by real-time qPCR quantification of *C rodentium* in fecal samples against standard curve generated from known numbers per colony-forming units of bacteria (Figure 6E).

Altered Mucosal B-Cell Function in I-Ab$^{\Delta IEC}$ Mice

We compared the colonic transcriptome of I-Ab^{WT} and I-Ab$^{\Delta IEC}$ mice at steady-state using whole genome microarray analysis. I-Ab$^{\Delta IEC}$ mice showed significantly different expression of 330 genes, with the most striking decrease in immunoglobulin mRNAs containing several heavy chain variable regions (Figure 7A). This observation, derived from hybridization-

based data, could either indicate true change in mRNA levels, or point to altered B-cell maturation and somatic hypermutation (SHM) normally occurring in the intestinal LP in response to dietary and microbial antigens. We used flow cytometry to determine the relative number of IgA-coated bacteria in the ileum of untreated mice, as a measure of IgA secretion and opsonization. We observed a significantly smaller pool of SIgA-coated bacteria in I-Ab$^{\Delta IEC}$ mice (Figure 7B). Although ELISA for total (not shown) and SIgA identified no significant difference among the 2 strains at steady-state (Figure 7C), we observed extremely low SIgA level in fecal content of *C rodentium*–infected I-Ab$^{\Delta IEC}$ mice as compared with infected I-Ab^{WT} controls. The greatest decrease in fecal SIgA was observed on day 9 postinfection, the period of highest expansion of *C rodentium* in I-Ab$^{\Delta IEC}$ mice (Figure 7D). This observation is consistent with the reported role of IgA in constraining the early expansion of *C rodentium* in mice.[27] FACS analysis of 2×10^8 colony-forming units of *C rodentium* reacted in vitro with the same concentrations of ileal showed diminished *C rodentium* specific reactivity of SIgA from I-Ab$^{\Delta IEC}$ mice (Figure 7E).

We next tested the frequency of CD138$^+$IgA$^+$ plasma cells from PPs as well as the small intestinal LP. We found a trend toward lower frequency of these cells in PP, but not in LP (data not shown) of I-Ab$^{\Delta IEC}$ mice as compared with I-Ab^{WT} and the absolute numbers of plasma cells in PP of I-Ab$^{\Delta IEC}$ mice was lower (Figure 7F). Although this change did not translate to an altered luminal SIgA concentration at baseline, decreased numbers of IgA-secreting plasma cells may have contributed to lower IgA levels during infection. We also verified that the mucosal expression of the polymeric Ig receptor was not altered in I-Ab$^{\Delta IEC}$ mice as determined by qRT-PCR and Western blotting (data not shown). We further tested whether the impaired IgA coating of commensals and *C rodentium* in I-Ab$^{\Delta IEC}$ mice was the result of a reduced diversity of the IgA repertoire. However, we found very limited differences in the BCR repertoire between 2 genotypes as defined by CDR3 region length, V gene usage, and the number of somatic mutations in the flow-sorted CD138$^+$IgA$^+$ plasma cells from PP and LP (Supplementary Figure 5). When we analyzed the CDR3 region length (expressed as coded amino acids) in bins ranging from 6–23aa, we again found no statistically significant difference in the relative sequence abundances (Supplementary Figure 5A). The number of somatic mutations per region was generally very similar between the genotypes except for the CDR2 region, which was significantly more mutated in the LP B cells of I-Ab$^{\Delta IEC}$ mice (Supplementary Figure 5B). The number of VH mutations per clonotype was not different (Supplementary Figure 5C). V gene utilization was similar in both LP and PP of I-Ab^{WT} or I-Ab$^{\Delta IEC}$ mice with the exception of the IGHV1S56*1 gene, which was used at approximately a 3-fold higher frequency by I-Ab$^{\Delta IEC}$ mice (Supplementary Figure 5D).

16S Amplicon Profiling of the IgA-coated Bacteria

Combined flow sorting and 16S amplicon profiling has been used to assess the functionality and specificity of IgA in targeting bacteria.[28,29] We used a similar approach to test for potential differences in commensal recognition by SIgA in I-Ab^{WT} and I-Ab$^{\Delta IEC}$ mice by 16S amplicon sequencing of flow-sorted IgA-coated bacteria from the ilea of both mouse strains. Two independent experiments were performed approximately 1 year apart, thus microbial drift in our colony accounts for some of the observed differences (in Figure

7G and H, we identified animals in each experiment as triangles or circles). The overall microbial alpha diversity of ileal microbiota was similar between I-Ab^{WT} and I-Ab$^{\Delta IEC}$ mice, regardless of the experiment (Figure 7G). The effects of microbial drift were more evident in Bray-Curtis dissimilarity analysis, in which experiment number was a more significant variable than genotype (ANOSIM, Figure 7H). The pattern of relative microbial abundance at the genus level confirmed this observation, where no genus reached statistical significance (Figure 7I). Overall, these results indicate that the specificity of IgA interactions is only weakly regulated by the epithelial MHCII, and the primary effect of epithelial MHCII deficiency was a decreased affinity of SIgA to commensal and pathogenic bacteria.

Discussion

Although several reports explored the role of IEC in “assisting” DCs in the maintenance of tolerance and homeostasis as nonprofessional APCs, it remains controversial whether they have a “direct” impact on mucosal tolerance or inflammation. To directly assess the contribution of IEC-expressed MHCII to mucosal homeostasis during intestinal inflammation, we developed I-Ab$^{\Delta IEC}$ mice with selective deficiency of MHCII in IEC. Importantly, I-Ab$^{\Delta IEC}$ mice did not develop spontaneous colitis, thus eliminating any confounding factors that could complicate data interpretation.

I-Ab$^{\Delta IEC}$ mice were modestly protected after DSS treatment, as demonstrated by less severe clinical parameters and reduced mucosal expression of inflammatory cytokines. Colonic and MLN effector T-cell activation appeared to be similar in I-Ab^{WT} and I-Ab$^{\Delta IEC}$ mice when compared with mice on regular drinking water. However, at baseline, we observed a tendency toward reduced numbers of induced Tregs in the cLP of I-Ab$^{\Delta IEC}$ mice, thus suggesting a modulatory role of IEC-MHCII on iTreg induction or maintenance. This is consistent with a TCR-HA model, where hemagglutinin presentation by primary IEC led to expansion of HA-specific CD4$^+$Foxp3$^+$Tregs.[21] On the other hand, unlike the I-Ab^{WT} mice, I-Ab$^{\Delta DEC}$ littermates did not show a significant reduction of mucosal CD4$^+$CD25$^+$Foxp3$^+$ Tregs during acute DSS colitis. Tregs promote the stem cell niche and self-renewal in the gut.[18] Thus, it is plausible that in the absence of intact MHCII on epithelial cells, exposure to microbial antigens better preserved the local Treg pool that subsequently conferred the observed modest protection and faster recovery from acute injury.

I-Ab$^{\Delta IEC}$ mice were also protected against naïve T-cell transfer colitis, most notably with respect to body weight recovery. This protection was associated with somewhat diminished accumulation of IFNγ-producing CD4$^+$T cells, suggesting that epithelial MHCII does contribute to the activation of Th1 responses. Indeed, in vitro studies based on coculture of human HT29 cells and intraepithelial lymphocytes from patients with IBD or healthy controls suggest that IEC can activate CD4$^+$T cells in MHCII-dependent fashion.[6] Mouse CEC (not stimulated to express MHCII) were unable to promote the activation of splenic CD4$^+$ T cells, but suppressed CD4$^+$ T-cell activation by macrophages.[14] Unlike IEC from small intestines, CECs do not express MHCII in steady-state[9] and need stimuli like IFNγ to up-regulate it. Our results suggest that up-regulation of MHCII on CEC by infiltrating Th1 cells may further promote Th1 responses.

During recovery from DSS and in T-cell transfer colitis, colonic mucosa of I-Ab$^{\Delta IEC}$ mice also produced more IL22, a cytokine that promotes mucosal healing and repair by inducing IEC activation and survival via STAT signaling[23] and promotes the expression of antimicrobial peptides such as RegIIIγ.[30] Because IL22 also mediates the early host defense against attaching and effacing bacterial pathogens,[31] we tested the role of epithelial MHCII in *C rodentium* infection. Epithelial MHCII was necessary to effectively control *C rodentium*, suggesting that the infected I-Ab$^{\Delta IEC}$ mice were not able to mount an effective immune response. Maggio-Price et al.[19] suggested that antigen presentation by DCs is sufficient to trigger severe bacteria-driven colitis. However, another study showed that mice that lacked IFNγ-inducible MHCII expression on all cells of nonhematopoietic lineages were susceptible to *Helicobacter hepaticus*–induced colitis.[20] In this context, our results highlight the role of epithelial MHCII expression in regulating susceptibility to enteric infection.

IgA is the most prominent antibody in the gut participating in pathogen and exotoxin neutralization, modulation of commensal microbiota, and mucosal inflammatory responses.[32,33] We observed decreased numbers of IgA^{+}CD138^{+} plasma cells in PP but not the small intestinal lamina propria of the I-Ab$^{\Delta IEC}$ mice as compared with I-Ab^{WT} littermates at steady-state. However, this did not correlate with differences in the luminal SIgA between 2 genotypes. Because the levels of luminal SIgA also reflect IgA induced in nonmucosal tissues, this discrepancy could be due to a compensation by hepatic SIgA.[34,35] It is also plausible that the contribution of T-cell–independent IgA production by LP B1b cells (nearly 40% of peritoneal B1 cell origin) is not modulated by epithelial MHCII and could contribute to total luminal SIgA concentration.[28,36] However, after *C rodentium* infection, SIgA secretion was reduced in I-Ab$^{\Delta IEC}$ mice relative to I-Ab^{WT} controls. Intestinal SIgA is a result of a consortium of different cells involved in antigen sampling, such as M cells present in follicle-associated epithelium, mononuclear phagocytes, and goblet cells.[37] It is plausible that the altered SIgA response was not a direct but an indirect consequence of ablation of IEC MHCII. Rios et al.[38] demonstrated that M cells have a critical and nonredundant role in driving SIgA responses specific to the commensal bacteria, deliver antigens to DCs that further interact with T follicular helper cells, and consequently lead to generation of memory B cells and plasma cells.[39] Recently, MHCII expression was demonstrated in Lgr5^{+} stem cells and IEC-specific deletion of MHCII resulted in depletion of the stem cell niche.[18] Because M cells also derive from Lgr5^{+} cells, it is also plausible that MHCII deletion in I-Ab$^{\Delta IEC}$ mice has affected the M-cell function leading to suboptimal antigen uptake and interaction with DCs and T_{fh} cells.

Most importantly, IgA coating of commensal bacteria in the gut of healthy I-Ab$^{\Delta IEC}$ mice was reduced, and SIgA from I-Ab$^{\Delta IEC}$ mice was less able to bind *C rodentium* in vitro. Thus, decreased SIgA and its decreased binding was likely responsible for increased susceptibility of I-Ab$^{\Delta IEC}$ mice to enteric infection. Although SHM is not a direct measure of IgA affinity, a thorough analysis of the BCR repertoire in PP and LP B cells found no meaningful differences in the V gene usage, the length, or mutations within CDR3 and other regions of IgA between the 2 genotypes, which could explain the difference in the “canonical” SIgA binding to intestinal bacteria. However, there are reports of “noncanonical” binding that is not affected by SHM and is primarily dependent on the

glycans associated with the constant chains of IgA.[40-42] SIgA is heavily glycosylated by IEC[43] with multiple glycans attached to hinge regions, secretory component, and J chain. Because free secretory component is known to interact with gut bacteria,[44] it seems plausible that IEC-specific MHCII influences the glycosylation and hence the noncanonical binding of IgA. It would be interesting, yet technically challenging, to investigate the IgA glycobiology in future studies.

Overall, our findings support a novel role of MHCII in the gut epithelia as a modulator of inflammatory responses to mucosal injury, T-cell–driven colitis, and enteric infection. Although epithelial MHCII promotes inflammatory responses and delays recovery in IBD-like models, it is required for an appropriate IgA-mediated response to mitigate enteric pathogen expansion and reduce mortality and morbidity in infection.

Supplementary Material

Refer to Web version on PubMed Central for supplementary material.

Funding

This work was supported by National Institutes of Health (NIH) 5R01 DK109711 (Pawel R. Kiela and Fayez K. Ghishan), PANDA Endowment in Autoimmune Diseases (Pawel R. Kiela), NIH RO1 DK108701 (Jean M. Wilson), and NIH R01 AI099108 (David G. Besselsen).

Transcript Profiling: (GEO Accession: GSE144952)

Abbreviations used in this paper:

APC	antigen presenting cell
CD	Crohn’s disease
CEC	colonic epithelial cell
cLP	colonic lamina propria
DC	dendritic cell
DSS	dextran sodium sulfate
ELISA	enzyme-linked immunosorbent assay
IBD	inflammatory bowel disease
IEC	intestinal epithelial cell
IFN	interferon
Ig	immunoglobulin
IL	interleukin
iTreg	induced Treg

MHC	major histocompatibility complex
MLN	mesenteric lymph node
mRNA	messenger RNA
qRT-PCR	quantitative reverse-transcriptase polymerase chain reaction
SHM	somatic hypermutation
SIgA	secretory IgA
TNF	tumor necrosis factor
Treg	regulatory T cell

References

1. Shao L, Serrano D, Mayer L. The role of epithelial cells in immune regulation in the gut. Semin Immunol 2001;13:163–176. [PubMed: 11394959]
2. Dotan I, Allez M, Nakazawa A, et al. Intestinal epithelial cells from inflammatory bowel disease patients preferentially stimulate CD4+ T cells to proliferate and secrete interferon-gamma. Am J Physiol Gastrointest Liver Physiol 2007;292:G1630–G1640. [PubMed: 17347451]
3. Mayer L, Eisenhardt D, Salomon P, et al. Expression of class II molecules on intestinal epithelial cells in humans. Differences between normal and inflammatory bowel disease. Gastroenterology 1991;100:3–12. [PubMed: 1983847]
4. Kaiserlian D, Vidal K, Revillard JP. Murine enterocytes can present soluble antigen to specific class II-restricted CD4+ T cells. Eur J Immunol 1989;19:1513–1516. [PubMed: 2570703]
5. Scott H, Solheim BG, Brandtzaeg P, et al. HLA-DR-like antigens in the epithelium of the human small intestine. Scand J Immunol 1980;12:77–82. [PubMed: 6997989]
6. Hoang P, Crotty B, Dalton HR, et al. Epithelial cells bearing class II molecules stimulate allogeneic human colonic intraepithelial lymphocytes. Gut 1992;33:1089–1093. [PubMed: 1398233]
7. Sanderson IR, Ouellette AJ, Carter EA, et al. Differential regulation of B7 mRNA in enterocytes and lymphoid cells. Immunology 1993;79:434–438. [PubMed: 7691725]
8. Fais S, Maiuri L, Pallone F, et al. Gliadin induced changes in the expression of MHC-class II antigens by human small intestinal epithelium. Organ culture studies with coeliac disease mucosa. Gut 1992;33:472–475. [PubMed: 1582589]
9. Chiba M, Iizuka M, Masamune O. Ubiquitous expression of HLA-DR antigens on human small intestinal epithelium. Gastroenterol Jpn 1988;23:109–116. [PubMed: 3290039]
10. Sarles J, Gorvel JP, Olive D, et al. Subcellular localization of class I (A,B,C) and class II (DR and DQ) MHC antigens in jejunal epithelium of children with coeliac disease. J Pediatr Gastroenterol Nutr 1987;6:51–56. [PubMed: 3540260]
11. Hirata I, Austin LL, Blackwell WH, et al. Immunoelectron microscopic localization of HLA-DR antigen in control small intestine and colon and in inflammatory bowel disease. Dig Dis Sci 1986;31:1317–1330. [PubMed: 3542442]
12. Nakazawa A, Watanabe M, Kanai T, et al. Functional expression of costimulatory molecule CD86 on epithelial cells in the inflamed colonic mucosa. Gastroenterology 1999;117:536–545. [PubMed: 10464129]
13. Borcherding F, Nitschke M, Hundorfean G, et al. The CD40-CD40L pathway contributes to the proinflammatory function of intestinal epithelial cells in inflammatory bowel disease. Am J Pathol 2010;176:1816–1827. [PubMed: 20133813]
14. Cruickshank SM, McVay LD, Baumgart DC, et al. Colonic epithelial cell mediated suppression of CD4 T cell activation. Gut 2004;53:678–684. [PubMed: 15082586]

15. Li XC, Almawi W, Jevnikar A, et al. Allogeneic lymphocyte proliferation stimulated by small intestine-derived epithelial cells. Transplantation 1995;60:82–89. [PubMed: 7624948]
16. Nakazawa A, Dotan I, Brimnes J, et al. The expression and function of costimulatory molecules B7H and B7-H1 on colonic epithelial cells. Gastroenterology 2004;126:1347–1357. [PubMed: 15131796]
17. Koyama M, Mukhopadhyay P, Schuster IS, et al. MHC Class II antigen presentation by the intestinal epithelium initiates graft-versus-host disease and is influenced by the microbiota. Immunity 2019;51:885–898.e7. [PubMed: 31542340]
18. Biton M, Haber AL, Rogel N, et al. T helper cell cytokines modulate intestinal stem cell renewal and differentiation. Cell 2018;175:1307–1320.e22. [PubMed: 30392957]
19. Maggio-Price L, Seamons A, Bielefeldt-Ohmann H, et al. Lineage targeted MHC-II transgenic mice demonstrate the role of dendritic cells in bacterial-driven colitis. Inflamm Bowel Dis 2013;19:174–184. [PubMed: 22619032]
20. Thelemann C, Eren RO, Coutaz M, et al. Interferon-gamma induces expression of MHC class II on intestinal epithelial cells and protects mice from colitis. PLoS One 2014;9:e86844. [PubMed: 24489792]
21. Westendorf AM, Fleissner D, Groebe L, et al. CD4+Foxp3+ regulatory T cell expansion induced by antigen-driven interaction with intestinal epithelial cells independent of local dendritic cells. Gut 2009;58:211–219. [PubMed: 18832523]
22. Bonelli M, Savitskaya A, Steiner CW, et al. Phenotypic and functional analysis of CD4+ CD25− Foxp3+ T cells in patients with systemic lupus erythematosus. J Immunol 2009;182:1689–1695. [PubMed: 19155519]
23. Pickert G, Neufert C, Leppkes M, et al. STAT3 links IL-22 signaling in intestinal epithelial cells to mucosal wound healing. J Exp Med 2009;206:1465–1472. [PubMed: 19564350]
24. Neurath MF. Cytokines in inflammatory bowel disease. Nat Rev Immunol 2014;14:329–342. [PubMed: 24751956]
25. Shah C, Hari-Dass R, Raynes JG. Serum amyloid A is an innate immune opsonin for Gram-negative bacteria. Blood 2006;108:1751–1757. [PubMed: 16735604]
26. Eckhardt ER, Witta J, Zhong J, et al. Intestinal epithelial serum amyloid A modulates bacterial growth in vitro and pro-inflammatory responses in mouse experimental colitis. BMC Gastroenterol 2010;10:133. [PubMed: 21067563]
27. Uren TK, Wijburg OL, Simmons C, et al. Vaccine-induced protection against gastrointestinal bacterial infections in the absence of secretory antibodies. Eur J Immunol 2005;35:180–188. [PubMed: 15593123]
28. Bunker JJ, Flynn TM, Koval JC, et al. Innate and adaptive humoral responses coat distinct commensal bacteria with immunoglobulin A. Immunity 2015;43:541–553. [PubMed: 26320660]
29. Palm NW, de Zoete MR, Cullen TW, et al. Immunoglobulin A coating identifies colitogenic bacteria in inflammatory bowel disease. Cell 2014;158:1000–1010. [PubMed: 25171403]
30. Kolls JK, McCray PB Jr, Chan YR. Cytokine-mediated regulation of antimicrobial proteins. Nat Rev Immunol 2008;8:829–835. [PubMed: 18949018]
31. Zheng Y, Valdez PA, Danilenko DM, et al. Interleukin-22 mediates early host defense against attaching and effacing bacterial pathogens. Nat Med 2008;14:282–289. [PubMed: 18264109]
32. Okai S, Usui F, Ohta M, et al. Intestinal IgA as a modulator of the gut microbiota. Gut Microbes 2017;8:486–492. [PubMed: 28384049]
33. Bunker JJ, Bendelac A. IgA responses to microbiota. Immunity 2018;49:211–224. [PubMed: 30134201]
34. Strugnell RA, Wijburg OL. The role of secretory antibodies in infection immunity. Nat Rev Microbiol 2010;8:656–667. [PubMed: 20694027]
35. Brown WR, Kloppel TM. The liver and IgA: immunological, cell biological and clinical implications. Hepatology 1989;9:763–784. [PubMed: 2651270]
36. Meyer-Bahlburg A B-1 cells as a source of IgA. Ann N Y Acad Sci 2015;1362:122–131. [PubMed: 26062045]

37. Schulz O, Pabst O. Antigen sampling in the small intestine. Trends Immunol 2013;34:155–161. [PubMed: 23083727]

38. Rios D, Wood MB, Li J, et al. Antigen sampling by intestinal M cells is the principal pathway initiating mucosal IgA production to commensal enteric bacteria. Mucosal Immunol 2016;9:907–916. [PubMed: 26601902]

39. Crotty S Follicular helper CD4 T cells (TFH). Annu Rev Immunol 2011;29:621–663. [PubMed: 21314428]

40. Briliute J, Urbanowicz PA, Luis AS, et al. Complex N-xglycan breakdown by gut *Bacteroides* involves an extensive enzymatic apparatus encoded by multiple co-regulated genetic loci. Nat Microbiol 2019;4:1571–1581. [PubMed: 31160824]

41. Nakajima A, Vogelzang A, Maruya M, et al. IgA regulates the composition and metabolic function of gut microbiota by promoting symbiosis between bacteriaS. J Exp Med 2018;215:2019–2034. [PubMed: 30042191]

42. Pabst O, Slack E. IgA and the intestinal microbiota: the importance of being specific. Mucosal Immunol 2020;13:12–21. [PubMed: 31740744]

43. Stadtmueller BM, Huey-Tubman KE, Lopez CJ, et al. The structure and dynamics of secretory component and its interactions with polymeric immunoglobulins. Elife 2016;5.

44. Mathias A, Corthesy B. N-Glycans on secretory component: mediators of the interaction between secretory IgA and gram-positive commensals sustaining intestinal homeostasis. Gut Microbes 2011;2:287–293. [PubMed: 22067937]

WHAT YOU NEED TO KNOW

BACKGROUND AND CONTEXT

Intestinal epithelial cells (IECs) provide a barrier that separates the mucosal immune system from the luminal microbiota. IECs constitutively express low levels of major histocompatibility complex (MHC) class II proteins, which are upregulated upon exposure to interferon gamma (IFNG).

NEW FINDINGS

In mice with DSS or T cell-induced colitis, loss of MHCII from IECs reduces but does not eliminate mucosal inflammation. However, in mice with *C rodentium*-induced colitis, loss of MHCII reduces bacterial clearance, by decreasing the affinity of IgA for commensal and pathogenic bacteria.

LIMITATIONS

This study was performed in mice; further studies of this immune response are needed in humans.

IMPACT

Strategies to modulate this pathway might be developed for treatment of inflammatory bowel diseases or enteric bacterial infections.

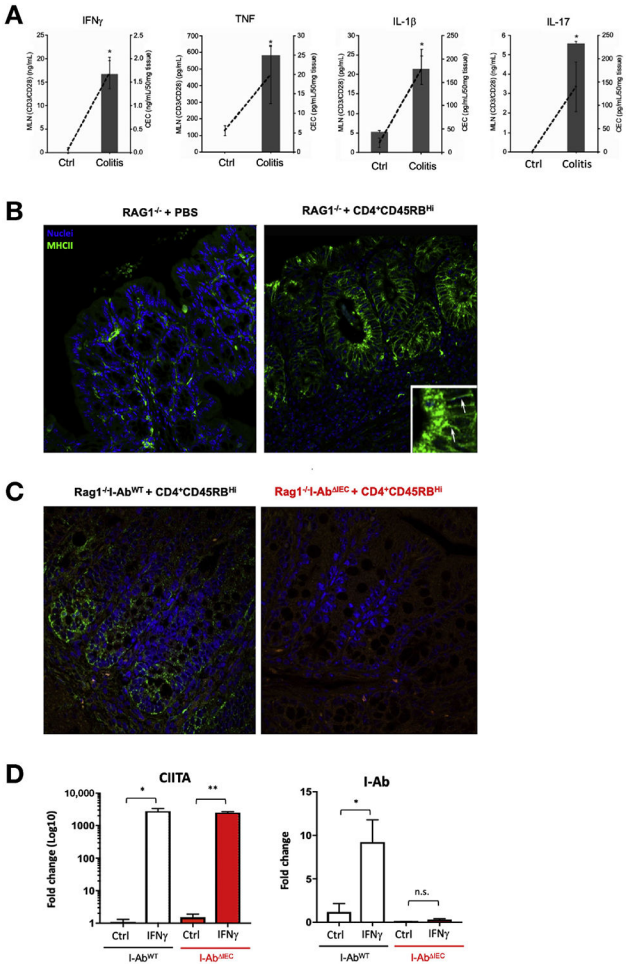

Figure 1.

Expression of MHCII in the colonic epithelium in adoptive T-cell transfer colitis. (*A*) Secretion of IFNγ, TNFα, IL1β, and IL17 by the CD3/CD28-stimulated MLN cells (*bars, left axis*) and by the colonic explants (*dashed line, right axis*). (*B*) Representative immunofluorescence imaging (n = 4). *Arrows* in the *magnified* inset show green MHCII signal. (*C* and *D*) MHCII ablation in I-Ab$^{\Delta IEC}$ mice. (*C*) Representative immunofluorescence of colonic sections (n = 8) showing complete loss of epithelial MHCII expression in adoptively transferred Rag1$^{-/-}$I-Ab$^{\Delta IEC}$ mice (*right*) as compared with Rag1$^{-/-}$I-Ab^{WT} mice (*left*). (*D*) qRT-PCR analysis of CIITA and I-Ab mRNA expression in control and IFNγ-stimulated (100 U/mL for 18 hours) colonoids prepared from I-Ab^{WT} and I-Ab$^{\Delta IEC}$ mice. TATA-box binding protein (TBP) was used as housekeeping gene. *Error bars* indicate standard deviation. *$P < .05$, **$P < .01$, Student *t* test.

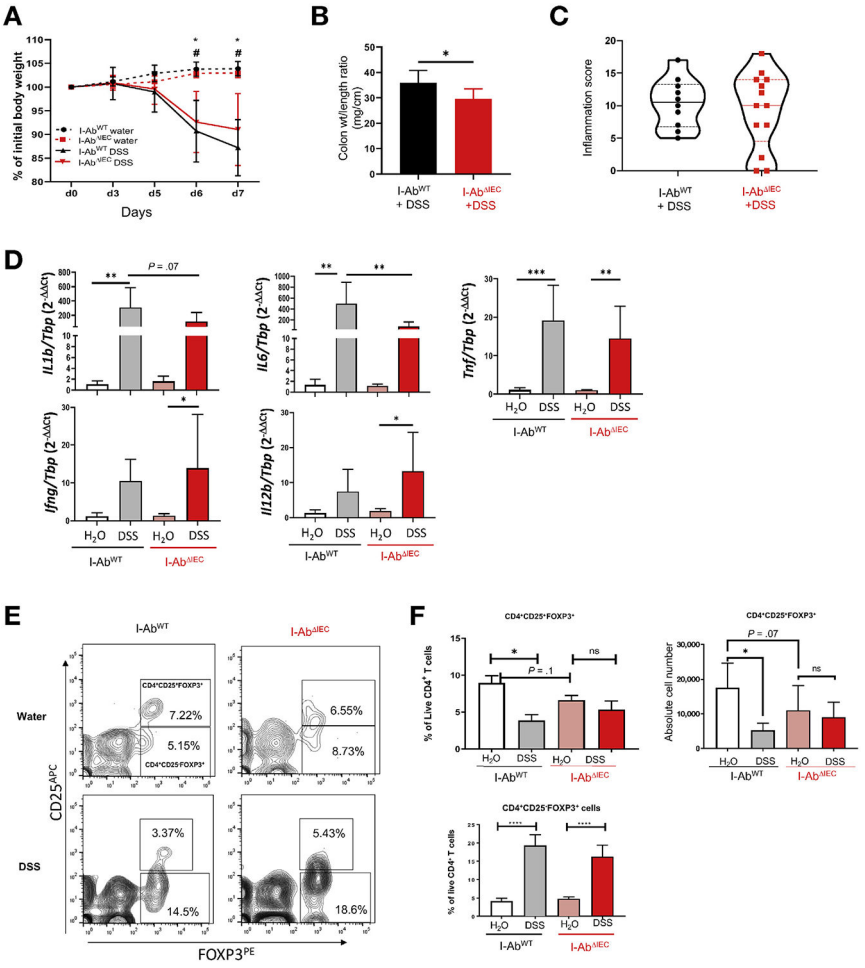

Figure 2.

Deletion of MHCII in IEC offers modest protection in acute DSS colitis. I-Ab^{WT} and I-Ab$^{\Delta IEC}$ mice were treated with 3% DSS in drinking water for 7 days. Data representative of 2 independent experiments (n = 10–13 mice in DSS group and n = 11–17 mice in H_2O group). (*A*) Weight loss expressed as percentage relative to the initial weight (*$P < .005$ or 0.001 H_2O vs DSS-treated I-Ab^{WT} mice on days 6 and 7, respectively; #$P < .005$ H_2O vs DSS-treated I-Ab$^{\Delta IEC}$ mice on days 6 and 7. (*B*) Colon length/weight ratio in DSS-treated mice. (*C*) Violin plot of the colonic inflammation score (solid lines indicate medians; dashed lines indicate quartiles). Slides were scored blindly, and total scores calculated as the sum of proximal and distal colon score. (*D*) qRT-PCR analysis of colonic IL1β, IL6, TNFα, IFNγ, and IL12b mRNA in I-Ab^{WT} and I-Ab$^{\Delta IEC}$ mice. Results expressed as relative expression normalized to TATA-box binding protein (TBP) mRNA. *$P < .05$, **$P < .01$, ****$P < .0001$ (1-way analysis of variance [ANOVA] followed by Bonferroni multiple comparison test). (*E*) Representative flow cytograms demonstrating the CD4$^+$CD25$^+$Foxp3$^+$ cells and CD4$^+$CD25$^-$Foxp3$^+$ regulatory T cells in the cLP of I-Ab^{WT} and I-Ab$^{\Delta IEC}$ mice. (*F*) Summary analysis of CD4$^+$CD25$^+$Foxp3$^+$ and CD4$^+$CD25$^-$Foxp3$^+$ cells in I-Ab^{WT} and I-Ab$^{\Delta IEC}$ on water or DSS. *$P < .05$, ****$P < .0001$ (1-way ANOVA followed by Bonferroni multiple comparison test).

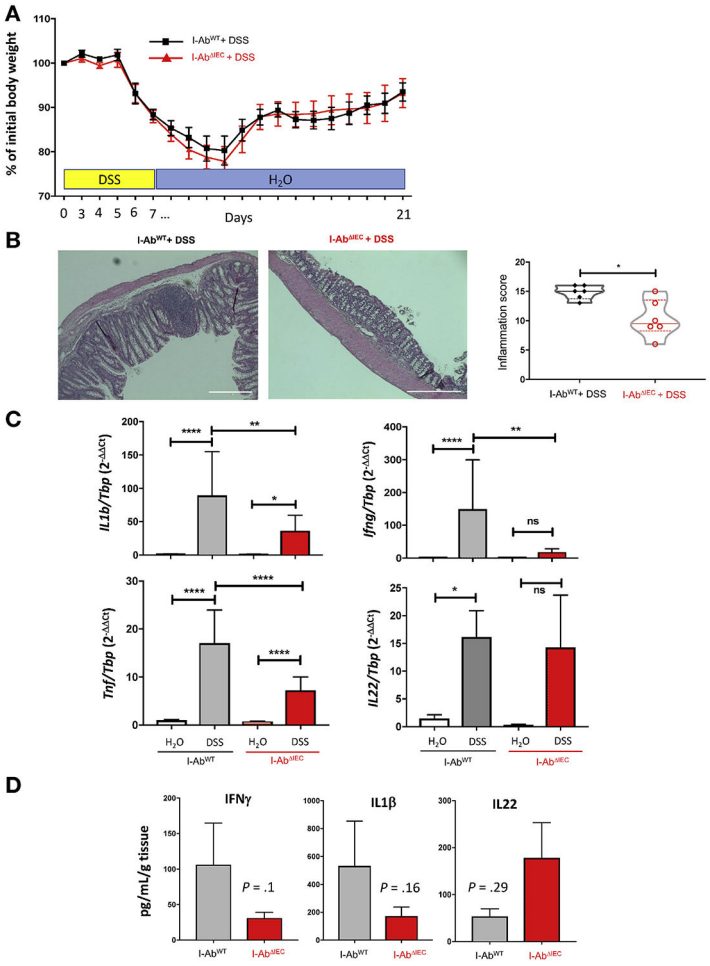

Figure 3.

Deletion of MHCII in IEC enhances mucosal restitution in DSS colitis. I-Ab^{WT} and I-Ab$^{\Delta IEC}$ mice were treated with 3% DSS in drinking water for 7 days and allowed to recover for 14 days. Data are representative of 2 independent experiments (n = 6 mice each in DSS group and n = 12–18 mice in H_2O group) (*A*) Weight loss displayed as percentage relative to the initial weight. (*B*) Representative hematoxylin-eosin images and violin plots of the colonic inflammation scores (*solid lines* indicate medians and *dashed lines* indicate quartiles). Total scores calculated as the sum of proximal and distal colon score (*$P < .05$, Student *t* test). (*C*) qRT-PCR analysis of colonic IL1β, IFNγ, TNFα, and IL22 mRNA in I-Ab^{WT} and I-Ab$^{\Delta IEC}$ mice. Results normalized to TATA-box binding protein (TBP) mRNA (*$P < .05$, **$P < .01$, ****$P < .0001$; 1-way analysis of variance followed by Bonferroni multiple comparison test). (*D*) IFNγ, IL1β, and IL22 secretion in colonic explant culture from I-Ab^{WT} (n = 3) and I-Ab$^{\Delta IEC}$ (n = 6) mice. Values normalized to dry weight of the colonic explants (pg/mL/g). *P* values from Student *t* test indicated.

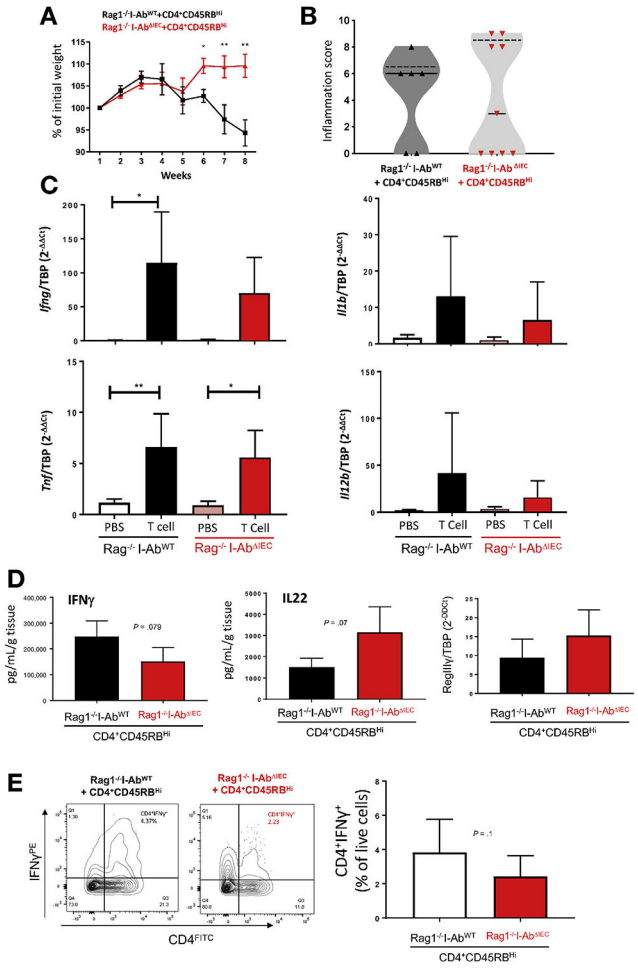

Figure 4.

Constitutive deletion of MHCII expression in IEC is protective in naive T-cell transfer colitis. Colitis was induced in Rag1$^{-/-}$I-Ab^{WT} and Rag1$^{-/-}$I-Ab$^{\Delta IEC}$ mice and monitored for 8 weeks. Data are representative of 2 independent experiments (n = 7–11 mice in each group). (*A*) Weight loss displayed as relative to the initial body weight. **P* < .05, ***P* < .01, Student *t* test. (*B*) Violin plots of the colonic inflammation scores (*solid lines* indicate medians and *dashed lines* indicate quartiles). (*C*) qRT-pCr analysis of colonic IL1β, IFNγ, TNFα, and IL12 mRNA in T-cell–transferred Rag1$^{-/-}$I-Ab^{WT} and Rag1$^{-/-}$I-Ab$^{\Delta IEC}$ mice. Results normalized to TATA-box binding protein (TBP) mRNA. Statistical significance calculated using 1-way analysis of variance followed by Bonferroni multiple comparison test. **P* < .05, ***P* < .01. (*D*) Cytokine secretion by colonic explants (Rag1$^{-/-}$I-Ab^{WT} n = 3, Rag1$^{-/-}$I-Ab$^{\Delta IEC}$ n = 4). *P* values of Student *t* test indicated. (*E*) Representative flow cytograms of IFNγ-producing CD4$^+$ T cells in CD3/CD28-simulated MLN cells. Percentage of CD4$^+$IFNγ^+ cells presented as the summary bar graph. *P* value of Student *t* test indicated.

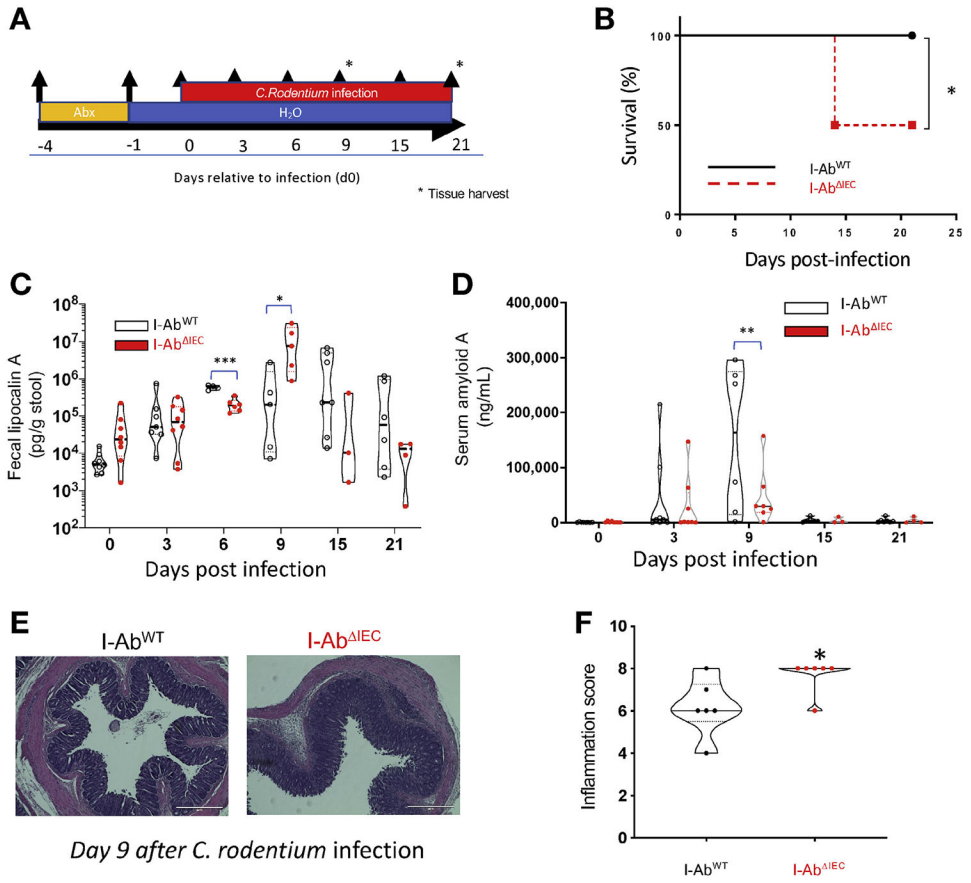

Figure 5.

1-Ab$^{\Delta IEC}$ mice are more susceptible to infectious colitis. Infectious colitis was induced in I-Ab^{WT} (n = 7) and I-Ab$^{\Delta IEC}$ (n = 8) by oral administration of *C rodentium* and followed for 21 days. (*A*) Experimental design timeline. (*B*) Survival curve: 50% of the I-Ab$^{\Delta IEC}$ mice died by day 15 postinfection (p.i.). (*C*) Fecal lipocalin 2 concentration measured by ELISA in longitudinally collected samples (*P < .01, ***P < .001, Student *t* test). (*D*) Serum amyloid A concentration measured by ELISA in longitudinally collected blood samples. **P < .01, Student *t* test. (*E*) Representative hematoxylin-eosin (H&E)-stained sections of colons on day 9 p.i. (*F*) Violin plots of the colonic inflammation score assessed blindly in H&E stained sections (*solid lines* indicate medians and *dashed lines* indicate quartiles); *P < .05.

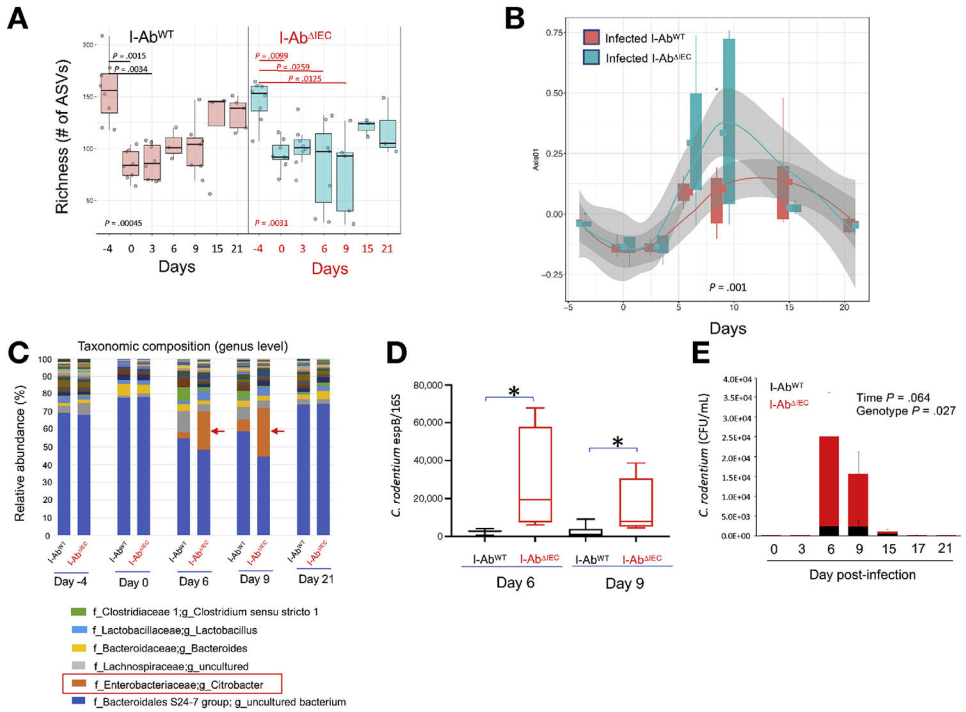

Figure 6.

16S ribosomal RNA amplicon profiling in *C rodenfium*–infected I-Ab^{WT} and I-Ab$^{\Delta IEC}$ mice. (*A*) Richness presented as the number of amplicon sequence variant (ASVs) was calculated in samples collected before (days −4 and 0) and after oral gavage with *C rodenfium* at indicated timepoints. Each box represents 75th and 25th percentile, *line* indicates the median, and *whiskers* indicate the extreme values. Kruskal-Wallis test *P* values are indicated. Bonferroni-adjusted *P* values above bars indicate statistically significant differences between timepoints calculated using Dunn's post hoc multiple comparison test. (*B*) Bray-Curtis dissimilarity (Axis 1) at the indicated time of collection. PERMANOVA (adonis) *P* value shown at the bottom of the plot. (*C*) Relative abundance of genera and (*D*) qPCR detection of *C rodentium* in fecal samples for day 6 and 9 postinfection using primers for espB gene and normalized against pan-16S qPCR for total bacteria. **P* < .05 Student *t* test. (*E*) Absolute qPCR quantification of *C rodentium* in fecal samples in I-Ab^{WT} and I-Ab$^{\Delta IEC}$ mice over time. Data were analyzed with mixed effects 2-way analysis of variance. *P* values for time and genotype as 2 fixed effects are indicated.

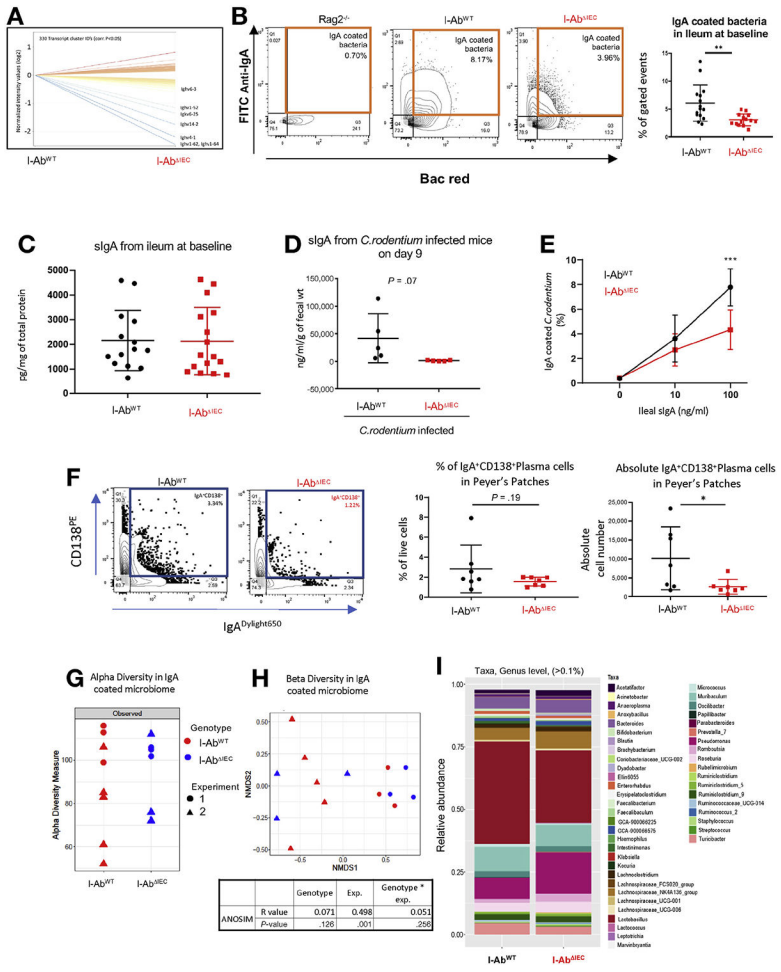

Figure 7.

(*A*) Microarray analysis of colonic gene expression from steady-state I-Ab^{WT} and I-Ab$^{\Delta IEC}$ mice (n = 3 each). Lines represent significantly up- or down-regulated genes and immunoglobulin heavy chain variable regions are highlighted. (*B*) Decreased frequency of IgA-coated bacteria I-Ab$^{\Delta IEC}$ mice. Ileal content from I-Ab^{WT} and I-Ab$^{\Delta IEC}$ mice was prepared, bacteria stained with Bac Red and anti-mouse IgA, and analyzed by flow cytometry. Rag1$^{-/-}$ mice were used as negative controls. Data are representative of 2 independent experiments (n = 8–10 mice in each group). Unpaired *t* test with Welch's correction, $^{**}P < .01$. (*C*) SIgA concentration in the ileum of healthy mice analyzed by ELISA. (*D*) SIgA concentration in the ilea of *C rodentium*–infected mice. (*E*) In vitro *C rodentium*–IgA binding assay. (*F*) Frequency and absolute numbers of CD138^{+}IgA^{+} plasma cells in Peyer's patches from I-Ab^{WT} and I-Ab$^{\Delta IEC}$ mice (n = 7 in each group, $^{*}P < .05$ Student *t* test). (*G-I*) 16S amplicon profiling of IgA-coated bacteria in the ilea of I-Ab^{WT} and I-Ab$^{\Delta IEC}$ mice (n = 6–8 in each group). (*G*) Richness (alpha diversity) was expressed as the number of ASVs. (*H*) Beta diversity analysis using Bray-Curtis dissimilarity-based nonmetric multidimensional scaling (NMDS). ANOSIM (Permutational Multivariate Analysis of Variance Using Distance Matrices) indicated a stronger effect of interexperimental variation (microbial drift), with no statistical difference between

genotypes. (*I*) Genus-level taxonomic analysis of IgA-coated bacteria. For clarity, all genera with a relative abundance <0.1% were filtered out.